Dalton Transactions

# New coordination networks containing trinuclear lanthanide complexes and hexacyanometallates



| | |
|---|---|
| Journal: | *Dalton Transactions* |
| Manuscript ID | DT-ART-07-2017-002541.R2 |
| Article Type: | Paper |
| Date Submitted by the Author: | 08-Apr-2018 |
| Complete List of Authors: | Escobedo-Cruz, Francisco; Texas A&M University , Chemistry<br>Hughbanks, Tim; Texas A&M University , Chemistry |
| | |

Journal Name

ARTICLE TYPE

Cite this: DOI: 10.1039/xxxxxxxxxx

# New coordination networks containing trinuclear lanthanide complexes and hexacyanometallates†

Francisco V. Escobedo-Cruz,*[a] and Tim R. Hughbanks[a]

Received Date
Accepted Date

DOI: 10.1039/xxxxxxxxxx

www.rsc.org/journalname

Three different families of trinuclear lanthanide complexes supported by TDCI (1,3,5-tris(dimethylamino)-1,3,5-trideoxy-cis-inositol), $[Ln_3(TDCI)_2(H_2O)]_6]^{3+}$, and hexacyanometallates as linkers have been synthesized and structurally characterized. The combination of $[Cr(CN)_6]^{3-}$ and trinuclear complexes having the ions $Gd^{3+}$, $Tb^{3+}$ and $Dy^{3+}$ results in a family of compounds that features 1D-chains that crystallize in the *Pmmn* space group. $[Fe(CN)_6]^{3-}$ couple with trinuclear complexes containing $Gd^{3+}$ - $Er^{3+}$ yields a family of compounds featuring 2D-networks that crystallize in the *Pnma* space group. Using $[Co(CN)_6]^{3-}$, a new family of compounds characterized by 1D-chains is obtained when the trinuclear cluster has the ions $Ho^{3+}$, $Er^{3+}$ and $Y^{3+}$, which crystallize in the *Pnma*. Magnetic susceptibility and magnetization measurements of selected compounds shows a magnetically independent behavior of their constituting ions with exception of $C_{30}H_{54}N_{12}O_9Er_3Fe$.

## 1 Introduction

The incorporation of rare-earth ions in the synthesis of new compounds has played an important role in obtaining new structures with properties that can be potentially applicable in diverse fields such as catalysis, optics and magnetism.[1–6] A strategy that has become widely employed consists of using rare-earth ions with blocking ligands and metal complexes as linkers to synthesize heterometallic coordination compounds,[7–11] and polycyano complexes have been one of the most commonly employed linkers.[7,12–15] Using metallocyanates as linkers offers the opportunity of using them as prebuilding blocks, and in combination with rare-earth ions, they tend to form cyano-bridged networks.[16–21]

In this study, we have exploited the hardness of the lanthanide ions and the affinity for hard ions of TDCI[22] or 1,3,5-tris(dimethylamino)-1,3,5-trideoxy-cis-inositol (Figure 1a) to synthesize trinuclear lanthanide complexes as tectons[23–25] (Figure 1b). We strategically utilized hexacyanometallates as complementary tectons to the trinuclear lanthanide complexes to form new 3d-4f heteronuclear assemblies to study their magnetic behavior.

Three different families of compounds were found when utilizing hexacyanometallates as linkers and trinuclear lanthanide complexes supported by TDCI, $[Ln_3(TDCI)_2(H_2O)_6]^{3+}$, as building block. In this building block, the lanthanide ions are located at the vertices of a triangle, and TDCI acts as the blocking ligand capping the three lanthanide ions above an below the plane that contains the lanthanide ions. The alkoxide groups of the TDCI ligand bridge two lanthanide ions and coordination by the amino groups to the lanthanide ions constrains the available coordination sites for the linkers to coordinate. The two available coordination sites per lanthanide ion are occupied by water molecules as seen in Figure 1b, and these water molecules are subject to be displaced by other ligands.

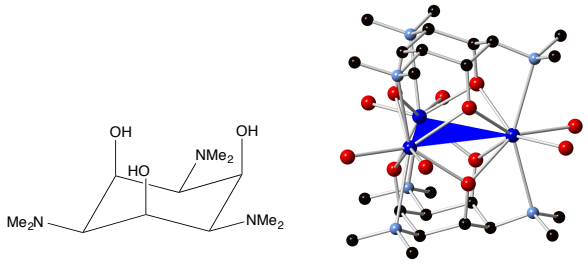


**(a)** TDCI **(b)** $[Ln_3(TDCI)_2(H_2O)_6]^{3+}$

**Fig. 1** (a) Ligand and (b) trinuclear complex, Ln ($Gd^{3+}$, $Tb^{3+}$, $Dy^{3+}$, $Ho^{3+}$, $Er^{3+}$, $Y^{3+}$) is depicted in blue, oxygen in red, nitrogen in light blue and carbon in black

In this paper, we discuss experimentation in which hexacyanometallates have been employed as bridging ligands and the magnetic behavior of selected compounds. The cyanido groups of the metallocyanates have shown to be capable of displacing coordinated water resulting in new coordination net-

[a] Department of Chemistry, Texas A&M, P.O. Box 30012, College Station, TX 77843-3255, USA. Fax: 979 845 8860; Tel: 979-845-0215; E-mail: TRH@chem.tamu.edu

† Electronic Supplementary Information (ESI) available: Crystallographic information is provided as CIF files for each compound. See DOI: 10.1039/b000000x/

**Table 1** Data collection and lattice parameters for $[Ln_3(TDCI)_2(H_2O)_4(\mu-CN)_2Cr(CN)_4]_n$

| Ln | Gd **(1)** | Tb **(2)** | Dy **(3)** |
|---|---|---|---|
| Formula | $C_{60}H_{112}O_{20}N_{24}Gd_6Cr_2$ | $C_{60}H_{112}O_{20}N_{24}Tb_6Cr_2$ | $C_{60}H_{112}O_{20}N_{24}Dy_6Cr_2$ |
| $F_w$ (g/mol) | 2537.22 | 2547.24 | 2568.72 |
| Crystal system | Orthorhombic | Orthorhombic | Orthorhombic |
| Space group | *Pmmn* | *Pmmn* | *Pmmn* |
| Z | 2 | 2 | 2 |
| a (Å) | 14.419(6) | 14.280(5) | 14.335(13) |
| b (Å) | 13.366(6) | 13.311(4) | 13.289(13) |
| c (Å) | 13.772(6) | 13.873(5) | 13.888(13) |
| V (Å$^3$) | 2654.2(19) | 2637.0(15) | 2646(4) |
| Abs. coefficient (mm$^{-1}$) | 3.950 | 4.226 | 4.439 |
| No. Reflection | | | |
| Collected | 25425 | 29281 | 139241 |
| Independent | 2533 | 3033 | 6322 |
| R indexes [I> $2\sigma$(I)] | $R_1^a$ = 0.0163 | $R_1^a$ = 0.0155 | $R_1^a$ = 0.0249 |
| | $wR_2^b$ = 0.0404 | $wR_2^c$ = 0.0433 | $wR_2^d$ = 0.0564 |
| R indexes (all data) | $R_1^a$ = 0.0181 | $R_1^a$ = 0.0167 | $R_1^a$ = 0.0357 |
| | $wR_2^b$ =0.0413 | $wR_2^c$ = 0.0442 | $wR_2^d$ = 0.0607 |
| Goodness of fit on $F^2$ | 1.041 | 1.090 | 1.052 |

$R_1^a = \sum||F_o|-|F_c||/\sum|F_o|$; $wR_2^{b,c,d} = \sum([w(F_o^2-F_c^2)^2]/\sum[(F_o^2)^2])^{1/2}$

works. With the aim of obtaining extended networks, the potassium salt of three different hexacyanometallates were employed: $[Cr(CN)_6]^{3-}$, $[Fe(CN)_6]^{3-}$ and $[Co(CN)_6]^{3-}$. Even though the molecular shape of the linkers is octahedral and have the same charge, substantial structural differences were observed as the identity of the hexacyanometallate was varied. For instance, with $[Cr(CN)_6]^{3-}$, chains composed of alternating units of trinuclear lanthanide complex and linker are obtained; with $[Fe(CN)_6]^{3-}$, a two dimensional sheet was observed. Even though $[Co(CN)_6]^{3-}$ also gives chain-based compounds similar to those obtained with $[Cr(CN)_6]^{3-}$, the compounds are still distinctly different. Additionally, the magnetic studies performed revealed the nature of the magnetic interactions among the lanthanide ions and the transition metals ions in the families of compounds studied.

## 2 Experimental

### 2.1 Starting materials

All of the reagents were utilized as received from commercial sources. The lanthanide triflates were synthesized by reacting triflic acid and lanthanide oxides in excess, which was later removed by vacuum filtration. Then the solution was heated to dryness, and the resulting solid was heated under dynamic vacuum at ~200°C for 48 hr to obtain the anhydrous salts. The synthesis of the ligand TDCI was obtained from phloroglucinol following the procedure previously reported.[26,27]

### 2.2 Synthesis of $[Ln_3(TDCI)_2(H_2O)_6](F_3CSO_3)_3$

The ligand TDCI (0.38 mmol) was placed in a test tube and water was slowly added until the ligand was completely dissolved. In a separate test tube 0.68 mmol (20% excess) of $Ln(F_3CSO_3)_3$ (Ln = $Gd^{3+}$, $Tb^{3+}$, $Dy^{3+}$, $Ho^{3+}$, $Er^{3+}$ and $Y^{3+}$) were placed and water was added until complete dissolution. The TDCI solution was added to the $Ln(F_3CSO_3)_3$ solution, and then the test tube was heated in an oil bath with constant stirring and under a stream of $N_2$ gas. Once crystals were observed, the test tube was removed from the oil bath and allowed to cool. Lastly, the crystals of the lanthanide complexes were collected and allowed to air dry.

### 2.3 Synthesis of $[Ln_3(TDCI)_2(H_2O)_{6-x}(\mu-CN)_xM(CN)_{6-x}]$

All of the compounds were synthesized by slow diffusion of solutions containing stoichiometric amounts of the reactants. In a vial, 0.0092 mmoles of $K_3[M(CN)_6]$ (M = Cr, Fe and Co) were dissolved in 1 mL of water in a vial and then 1 mL of acetonitrile was added. A 4-mL solution of water:acetonitrile:ethanol in a volume ratio of 1:1:2 was carefully placed on top of the solution containing the hexacyanometallate. Lastly, a 2-mL layer of an ethanolic solution ($4.6\times10^{-3}$ M) of the trinuclear lanthanide complex was placed. After two weeks crystals suitable for X-Ray diffraction were obtained. The final mass of the crystals was determined by extracting the crystals soaked in the mother liquor, and then they were dry under vacuum. Then a portion of the crystals were analyzed by TGA and determined the dry mass of the compounds. The yields for the reaction varied in a range between 40 - 50 %.

### 2.4 X-Ray Data Collection

Single crystal X-Ray data was collected with a Bruker-AXS APEXII equipped with Three-Circle D5000 Goniometer and CCD/Phosphor Mo$K_\alpha$ X-ray radiation ($\lambda = 0.71073$Å). Single crystals of each of the compounds were mounted on nylon loops and placed under $N_2$ stream at 150 K for data collection. Indexing and data integration were carried out using APEX2 Software Suite of programs.[28] The program SADABS was utilized for absorption corrections.[29] For structure elucidation, OLEX$^2$ version 1.2.5 software[30] was used as the interface to SHELXS to solve the structures with Direct Methods and to SHELXL to refine the structures with the Least-Squares method.[31] A solvent mask was employed in order to reduce the disorder introduced by the solvent molecules and to give some homogeneity to the structure refinement for the compounds within the same families since the solvent molecules were partially resolved for each of the compounds but varied from compound to compound.

**Table 2** Data collection and lattice parameters for $[Ln_3(TDCI)_2(H_2O)_3(\mu-CN)_3Fe(CN)_3]_n$

| Ln | Gd **(4)** | Tb**(5)** | Dy **(6)** | Ho **(7)** | Er **(8)** |
|---|---|---|---|---|---|
| Formula | $C_{120}H_{216}O_{36}N_{48}Gd_{12}Fe_4$ | $C_{120}H_{216}O_{36}N_{48}Tb_{12}Fe_4$ | $C_{120}H_{216}O_{36}N_{48}DY_{12}Fe_4$ | $C_{120}H_{216}O_{36}N_{48}Ho_{12}Fe_4$ | $C_{120}H_{216}O_{36}N_{48}Er_{12}Fe_4$ |
| $F_w$ (g/mol) | 5017.80 | 5037.84 | 5080.8 | 5109.96 | 4993.92 |
| Crystal system | Orthorhombic | Orthorhombic | Orthorhombic | Orthorhombic | Orthorhombic |
| Space group | *Pnma* | *Pnma* | *Pnma* | *Pnma* | *Pnma* |
| Z | 4 | 4 | 4 | 4 | 4 |
| a (Å) | 16.401(4) | 16.359(3) | 16.325(2) | 16.276(3) | 16.239(4) |
| b (Å) | 18.919(4) | 18.917(3) | 18.887(3) | 18.779(3) | 18.833(4) |
| c (Å) | 14.122(3) | 14.106(2) | 14.075(2) | 14.043(3) | 14.043(3) |
| V (Å$^3$) | 4381.9(16) | 4365.1(13) | 4339.6(11) | 4292.2(13) | 4294.8(17) |
| Abs. coefficient (mm$^{-1}$) | 4.865 | 5.186 | 5.493 | 5.862 | 6.193 |
| No. Reflection | | | | | |
| Collected | 36000 | 37251 | 38945 | 29300 | 39578 |
| Independent | 3240 | 3353 | 3554 | 2477 | 3633 |
| R indexes [I> $2\sigma$(I)] | $R_1^a = 0.0282$ | $R_1^a = 0.0259$ | $R_1^a = 0.0226$ | $R_1^a = 0.0234$ | $R_1^a = 0.0261$ |
| | $wR_2^b = 0.0582$ | $wR_2^c = 0.0528$ | $wR_2^d = 0.0453$ | $wR_2^e = 0.0529$ | $wR_2^f = 0.0545$ |
| R indexes (all data) | $R_1^a = 0.0369$ | $R_1^a = 0.0340$ | $R_1^a = 0.0274$ | $R_1^a = 0.0269$ | $R_1^a = 0.0335$ |
| | $wR_2^b = 0.0611$ | $wR_2^c = 0.0586$ | $wR_2^d = 0.0468$ | $wR_2^e = 0.0545$ | $wR_2^f = 0.0575$ |
| Goodness of fit on $F^2$ | 1.051 | 1.048 | 1.035 | 1.077 | 1.031 |

$R_1^a = \sum ||F_o| - |F_c|| / \sum |F_o|$; $wR_2^{b,c,d} = \sum([w(F_o^2 - F_c^2)^2] / \sum[(F_o^2)^2])^{1/2}$

**Table 3** Data collection and lattice parameters for $[Ln_3(TDCI)_2(H_2O)_4(\mu-CN)_2Co(CN)_4]_n$

| Ln | Ho **(9)** | Er **(10)** | Y **(11)** |
|---|---|---|---|
| Formula | $C_{120}H_{224}O_{40}N_{48}Ho_{12}Co_4$ | $C_{120}H_{224}O_{40}N_{48}Er_{12}Co_4$ | $C_{120}H_{224}O_{40}N_{48}Y_{12}Co_4$ |
| $F_w$ (g/mol) | 5194.32 | 5222.28 | 4282.08 |
| Crystal system | Orthorhombic | Orthorhombic | Orthorhombic |
| Space group | *Pnma* | *Pnma* | *Pnma* |
| Z | 4 | 4 | 4 |
| a (Å) | 24.606(5) | 24.591(9) | 24.568(14) |
| b (Å) | 12.873(2) | 12.863(5) | 12.893(7) |
| c (Å) | 16.083(3) | 16.091(6) | 16.127(9) |
| V (Å$^3$) | 5094.3(16) | 5090(3) | 5109(5) |
| Abs. coefficient (mm$^{-1}$) | 4.993 | 5.269 | 16.545 |
| Extinction coefficient | 4.982 | 5.269 | 3.752 |
| No. Reflection | | | |
| Collected | 44924 | 48261 | 57895 |
| Independent | 4109 | 4591 | 5815 |
| R indexes [I> $2\sigma$(I)] | $R_1^a = 0.0208$ | $R_1^a = 0.0301$ | $R_1^a = 0.0309$ |
| | $wR_2^b = 0.0489$ | $wR_2^c = 0.0670$ | $wR_2^d = 0.0772$ |
| R indexes (all data) | $R_1^a = 0.0264$ | $R_1^a = 0.0414$ | $R_1^a = 0.0397$ |
| | $wR_2^b = 0.0511$ | $wR_2^c = 0.0710$ | $wR_2^d = 0.0808$ |
| Goodness of fit on $F^2$ | 1.045 | 1.061 | 1.051 |

$R_1^a = \sum ||F_o| - |F_c|| / \sum |F_o|$; $wR_2^{b,c,d} = \sum([w(F_o^2 - F_c^2)^2] / \sum[(F_o^2)^2])^{1/2}$

#### 2.4.1 X-Ray Diffraction Studies of $[Ln_3(TDCI)_2(H_2O)_4Cr(\mu-CN)_2(CN)_4]_n$

For $[Gd_3(TDCI)_2(H_2O)_4(\mu-CN)_2Cr(CN)_4]_n$, a pale yellow needle crystal with dimension 0.034 x 0.103 x 0.989 $mm^3$ was placed on the diffractometer and 25344 reflections were collected. For $[Tb_3(TDCI)_2(H_2O)_4(\mu-CN)_2Cr(CN)_4]_n$, a pale yellow crystal with dimension 0.026 x 0.045 x 0.64 $mm^3$ was placed on the diffractometer and 28983 reflections were collected. Also, for $[Dy_3(TDCI)_2(H_2O)_4(\mu-CN)_2Cr(CN)_4]_n$ a pale yellow needle crystal with dimension 0.028 x 0.054 x 0.712 $mm^3$ was placed on the diffractometer and 140506 reflections were collected. The lattice parameters, the crystallographic data collection and refinement parameters are given in Table 1.

#### 2.4.2 X-Ray Diffraction Studies of $[Ln_3(TDCI)_2(H_2O)_3(\mu-CN)_3Fe(CN)_3]_n$

For $[Gd_3(TDCI)_2(H_2O)_3(\mu-CN)_3Fe(CN)_3]_n$, an orange trapezoidal crystal with dimension 0.049 x 0.057 x 0.118 $mm^3$ was placed on the diffractometer and 36070 reflections were collected. For $[Tb_3(TDCI)_2(H_2O)_3(\mu-CN)_3Fe(CN)_3]_n$, also an orange trapezoidal crystal with dimension 0.042 x 0.082 x 0.127 $mm^3$ was placed on the diffractometer and 37409 reflections were collected. For the analogous compound $[Dy_3(TDCI)_2(H_2O)_3(\mu-CN)_3Fe(CN)_3]_n$, also an orange crystal with dimension 0.048 x 0.073 x 0.121 $mm^3$ was placed on the diffractometer and 39086 reflections were collected. For $[Ho_3(TDCI)_2(H_2O)_3(\mu-CN)_3Fe(CN)_3]_n$, an orange trapezoidal crystal with dimension 0.056 x 0.067 x 0.132 $mm^3$ was placed on the diffractometer and 29262 reflections were collected. Lastly, for $[Er_3(TDCI)_2(H_2O)_3(\mu-CN)_3Fe(CN)_3]_n$, also an orange trapezoidal crystal with dimension 0.045 x 0.057 x 0.110 $mm^3$ was placed on the diffractometer and 39627 reflections were collected. The lattice parameters, the crystallographic data collection and refinement parameters are given in Table 2.

#### 2.4.3 X-Ray Diffraction Studies of $[Ln_3(TDCI)_2(H_2O)_4Co(\mu-CN)_2(CN)_4]_n$

For $[Ho_3(TDCI)_2(H_2O)_4(\mu-CN)_2Co(CN)_4]_n$, a lightly pink flat needle crystal with dimension 0.032 x 0.041 x 0.521 $mm^3$ was placed on the diffractometer and 44784 reflections were collected. For $[Er_3(TDCI)_2(H_2O)_4(\mu-CN)_2Co(CN)_4]_n$, a flat needle crystal with dimension 0.027 x 0.038 x 0.461 $mm^3$ was placed on the diffractometer and 47990 reflections were collected, and for $[Y_3(TDCI)_2(H_2O)_4(\mu-CN)_2Cr(CN)_4]_n$, a colorless flat needle crystal with dimension 0.024 x 0.032 x 0.312 $mm^3$ was placed on the diffractometer and 58398 reflections were collected. The lattice parameters, the crystallographic data collection and refinement parameters are given in Table 3.

### 2.5 Magnetic susceptibility measurements

Magnetic susceptibility and magnetization measurements were performed on selected polycrystalline samples of the compounds **(1)**, **(2)**, **(3)**, **(6)**, **(7)** and **(8)**. The magnetic susceptibility measurements and magnetization were performed using a Quantum Design SQUID magnetometer MPMS-3. Magnetic susceptibility measurements were obtained by applying a magnetic field of 1000 Oe at 2 - 10 K intervals in a temperature range of 2 - 300 K. Magnetization measurements were performed at 1.8 K by applying a magnetic field from 0.05 - 7 T. The data obtained was corrected after the measurements for the diamagnetic contribution of the solvent and constituent atoms using Pascal's constants.[32]

## 3 Results and Discussion

### 3.1 Synthesis

The initial conditions for the synthesis of the hexacyanometallates were using the solvents water and ethanol in a ratio 1:1. The linker was dissolved in water and the trinuclear lanthanide complex in ethanol; however, the crystals obtained did not possess the quality necessary to obtain good crystal refinements. By reducing the amount of water to half of the original and adding acetonitrile, as described in the experimental section, better crystals were obtained. The three hexacyanometallates, $K_3[M(CN)_6]$ (M = $Cr^{3+}$, $Fe^{3+}$ and $Co^{3+}$) were combined with the trinuclear lanthanide complexes $[Ln_3(TDCI)_2(H_2O)_6](F_3CSO_3)_3$, (Ln = $Gd^{3+}$, $Tb^{3+}$, $Dy^{3+}$, $Ho^{3+}$, $Er^{3+}$ and $Y^{3+}$), but not all of them produced crystals. When using the linker $[Cr(CN)_6]^{3-}$, crystals suitable for single crystal X-Ray diffraction were obtained only when the trinuclear lanthanide complexes had $Gd^{3+}$, $Tb^{3+}$ or $Dy^{3+}$. However, when the trinuclear lanthanide complexes had $Ho^{3+}$, $Er^{3+}$ or $Y^{3+}$, crystals were not observed, but a layer resembling small portion of a cotton ball was formed. The linker $[Co(CN)_6]^{3-}$, in contrast, gave good crystals only with the trinuclear lanthanide complexes containing $Ho^{3+}$, $Er^{3+}$ and $Y^{3+}$, but it did not form crystals with trinuclear lanthanide complexes having $Gd^{3+}$, $Tb^{3+}$ or $Dy^{3+}$, instead a fuzzy layer was formed. $[Fe(CN)_6]^{3-}$ was the most versatile linker, as good crystals were obtained with trinuclear lanthanide complex containing $Gd^{3+}$, $Tb^{3+}$, $Dy^{3+}$, $Ho^{3+}$ and $Er^{3+}$. When the trinuclear lanthanide complex had Y, however, a fuzzy layer was obtained instead. The reaction of $[Cr(CN)_6]^{3-}$ with the trinuclear lanthanide complexes having Gd, Tb and Dy ions produced a family of three isostructural compounds that crystallized as pale yellow needles, $[Ln_3(TDCI)_2(H_2O)_4(\mu-CN)_2Cr(CN)_4]_n$. The combination of $[Fe(CN)_6]^{3-}$ and the trinuclear lanthanide complexes containing the ions $Gd^{3+}$ - $Ho^{3+}$ produced another family of five isostructural compounds that crystallized as flat orange trapezoids, $[Ln_3(TDCI)_2(H_2O)_3(\mu-CN)_3Fe(CN)_3]_n$. Lastly, the linker $[Co(CN)_6]^{3-}$ in combination with the trinuclear lanthanide complexex having the ions Ho, Er and Y resulted in another family of three isostructural compounds that crystallized as very pale yellow needles, $[Ln_3(TDCI)_2(H_2O)_4(\mu-CN)_2Co(CN)_4]_n$. All of the crystals were stable in the solvent for about two weeks, and after that period, the crystals slowly started to degrade to a fine powder. The crystals also decomposed when they were removed from the solvent; the compounds having the liker $[Fe(CN)_6]^{3-}$ decomposed faster than those containing the linker $[Cr(CN)_6]^{3-}$. The slow degradation of the crystals in the solvent is caused by the water molecules replacing the cyanido ligands from the linkers because of the oxophilicity of the lanthanide ions.

### 3.2 X-Ray Structure Studies

Even though the solvent molecules were partially resolved during the structure refinements for the compounds presented in this paper, there were still large displacement of atoms and unresolved peaks. The partial resolution of the solvent molecules for the compounds in the same family was not consistent; hence, a solvent mask was applied in order to solve refinement complications caused by the solvent molecules. When applying a solvent mask, the electron density in each of the solvent accessible voids (SAVs) for the compounds within the same family was consistent, and although ethanol and acetonitrile were also employed as solvents, the electron densities determined match better with water molecules. To illustrate the fact that water molecules are occupying the SAVs, compound **(10)** was resolved by applying a solvent mask without attempting to solve any of the water molecules, and the electron density in the SAVs was found to be $\approx 100$ $e^-$. Then, after only eight $H_2O$ molecules were resolved accurately for compound **(10)**, a solvent mask was applied and the remaining electron density was $\approx 20$ $e^-$, which is consistent with the electron count for two $H_2O$ molecules. Since the electron density for all of the compounds is consistent within each family, the third family of compounds presented is more accurately described as $C_{30}H_{56}O_{10}N_{14}Ln_3Co\cdot 10H_2O$ (Ln = $Ho^{3+}$, $Er^{3+}$ and $Y^{3+}$). For the second family each SAV has an electron count of $\approx 30$ $e^-$ or three water molecules, so this family can be described as $C_{30}H_{56}O_{10}N_{14}Ln_3Fe\cdot 3H_2O$ (Ln = $Gd^{3+}$, $Tb^{3+}$, $Dy^{3+}$, $Ho^{3+}$ and $Er^{3+}$). Even though the electron density for the first family of compounds was not as consistent, the electron densities found correspond to 8, 9 and 10 water molecules for compounds **(2)**, **(3)** and **(1)**, respectively.

#### 3.2.1 $[Ln_3(TDCI)_2(H_2O)_4Cr(\mu-CN)_2(CN)_4]_n$

The compounds in this familiy can be referred to as a copolymer in which the linker and trinuclear lanthanide complex are the alternating monomers, for it features alternating units of $[Cr(CN)_6]^{3-}$ and the trinuclear lanthanide complex $[Ln_3(TDCI)_2(H_2O)_4]^{3+}$ (Ln = $Gd^{3+}$, $Tb^{3+}$ and $Dy^{3+}$) as building blocks (Figure 2).

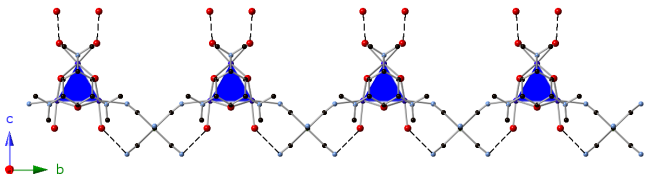


**Fig. 2** A portion of the $[Ln_3(TDCI)_2(H_2O)_4(\mu-CN)_2Cr(CN)_4]$ chain showing the hydrogen bonding, which is represented as dashed lines

Since the three compounds synthesized are isostructural, only compound **(2)** will be discussed, and the selected distances for the compounds in this family are summarized in Table 4. The $Tb^{3+}$ ions in the trinuclear lanthanide complex are located at the vertices of a triangle, and the ligand TDCI caps the $Tb^{3+}$ ions above and below the $Tb_3$ plane as shown in Figure 3. The $Tb(1)^{3+}$ ion is coordinated by four oxygen atoms from four $\mu$-alkoxo groups and by two amino groups of the ligand, by one water and by a cyanido group of the linker. The $\mu_2-O(2)-Tb(1)$ distance is 2.2914(12) Å, which is close to the distances of the Gd and Dy analogous compounds, 2.2836(15) and 2.2811(19) Å, respectively. For $\mu_2-O(3)-Tb(1)$, the distance is 2.3417(14) Å while for Gd and Dy, respectively, are 2.3349(17) and 2.336(2) Å, close to being constant across the three lanthanide compounds. The Tb(1) – N(4) (amine) distance is 2.6382(18) Å, and it can be consider the same for the Gd and Dy compounds, 2.633(2) and 2.634(4) Å, respectively. The bond distance of Tb(1)–O(1), water coordinated to the $Tb(1)^{3+}$, is 2.446(2) Å, and this distance is very similar to those in the Gd and Dy complexes. The Tb(1) – N(1) (CN group) distance is 2.476(3) Å, which is slightly shorter than the one previously reported,[5] but moderately larger than those for Gd and Dy, 2.465(3) and 2.463(4) Å, respectively.

The coordination around $Tb(2)^{3+}$ ion is similar to that of $Tb(1)^{3+}$ ion except that $Tb(2)^{3+}$ ion has two water molecules coordinated instead of a cyanido group, as shown in Figure 4. For $\mu_2-O(3)-Tb(2)$, the distance is 2.3230(14) Å which is close in value to the Gd analogous compound, 2.3194(17) Å, and the Dy-based compound, 2.3132(19) Å. The Tb(2)–O(4) distance is 2.423(3) Å, which is similar to those found in the Gd and Dy compounds. The slightly longer distances observed around the $Tb(2)^{3+}$ ion can be interpreted from this ion having two coordinated water molecules while $Tb(1)^{3+}$ ion has one water and a

**Table 4** $[Ln_3(TDCI)_2(H_2O)_4(\mu-CN)_2Cr(CN)_4]_n$: Selected distances (Å)

| Ln | Gd **(1)** | Tb **(2)** | Dy **(3)** |
|---|---|---|---|
| Ln(1) - Ln(1) | 3.6314(15) | 3.6421(12) | 3.627(4) |
| Ln(1) - Ln(2) | 3.7009(13) | 3.7028(10) | 3.692(3) |
| Ln(1) - O(1) | 2.418(3) | 2.446(2) | 2.430(3) |
| Ln(1) - O(2) | 2.2836(15) | 2.2914(12) | 2.2811(19) |
| Ln(1) - O(3) | 2.3349(17) | 2.3417(14) | 2.336(2) |
| Ln(1) - N(1) | 2.465(3) | 2.476(3) | 2.463(4) |
| Ln(1) - N(4) | 2.633(2) | 2.6382(18) | 2.634(3) |
| Ln(2) - O(3) | 2.3194(17) | 2.3230(14) | 2.3132(19) |
| Ln(2) - O(4) | 2.391(3) | 2.423(3) | 2.404(4) |
| Ln(2) - N(5) | 2.636(3) | 2.648(3) | 2.646(4) |
| C(1) - N(1) | 1.161(5) | 1.151(4) | 1.153(4) |
| C(2) - N(2) | 1.145(5) | 1.152(4) | 1.150(5) |
| C(3) - N(3) | 1.154(5) | 1.150(4) | 1.152(5) |
| Cr(1) - C(1) | 2.070(4) | 2.070(3) | 2.073(3) |
| Cr(1) - C(2) | 2.069(5) | 2.068(4) | 2.076(4) |
| Cr(1) - C(3) | 2.082(4) | 2.076(3) | 2.078(4) |
| | N···O hydrogen bond distances (Å) | | |
| N(3) - O(1) | 3.076(5) | 3.097(3) | 3.119(4) |

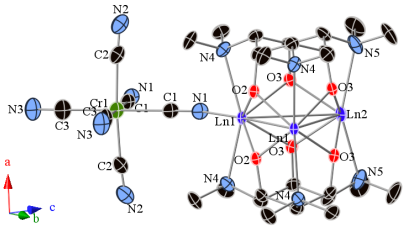


**Fig. 3** $[Ln_3(TDCI)_2(H_2O)_4(\mu-CN)_2Cr(CN)_4]$: ORTEP drawing with 50% probability, water molecules omitted for clarity

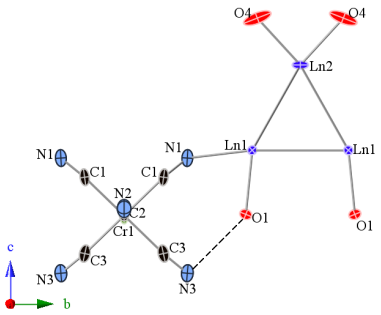


**Fig. 4** ORTEP drawing with 50% probability of $[Ln_3(TDCI)_2(H_2O)_4(\mu-CN)_2Cr(CN)_4]$ without the ligand TDCI

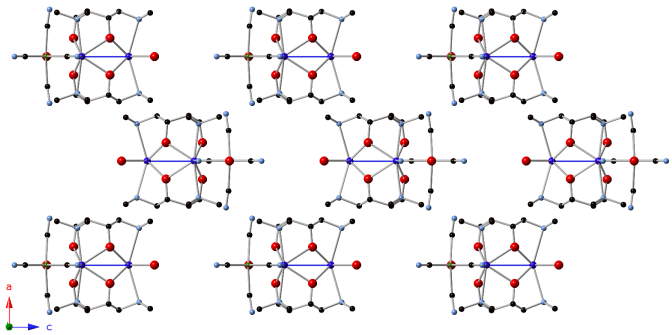


**Fig. 5** $[Ln_3(TDCI)_2(H_2O)_4(\mu-CN)_2Cr(CN)_4]_n$: View through the b-axis

cyanido ligand coordinated. Since the cyanido ligand is not as good electron donor as water, the alkoxo and amino groups from TDCI and the coordinated water molecule around $Tb(1)^{3+}$ move closer to donate more electron density causing the alkoxo and amino groups from TDCI around $Tb(2)^{3+}$ move further causing an elongation of the bond distances.

The $Cr^{3+}$ ion is coordinated by six cyanide groups forming a regular octahedron. The $Cr-C$ distances range from 2.068(8) to 2.082(4) Å, which are consistent with distances previously reported.[5] $[Cr(CN)_6]^{3-}$ connects two $[Tb_3(TDCI)_2(H_2O)_4]^{3+}$ building blocks through two cis equatorial cyanido groups, with $\angle Tb(1)N(1)C(1) = 147.1(6)^\circ$; the $Tb^{3+}$ ions of the trinuclear lanthanide complexes involved in the linkage, $Tb(1)^{3+}$ - $Tb(1)^{3+}$, can be seen as the base of the triangles. Each $[Cr(CN)_6]^{3-}$ unit bridges two trinuclear lanthanide complexes through the bases of the triangle formed by the $Tb^{3+}$ ions, thus, forming a 1-D chain of alternating units of linker and trinuclear lanthanide complex that grows along the *b axis*. The chains in this compound are also characterized by having hydrogen bonding of 'moderate' strength[33] between the water molecules coordinated to the $Tb^{3+}$ ions and the nitrogens from the cyanido groups, $d[N(3)\cdots O(1)] = 3.097(3)$ Å, as seen in Figure 4. The stacking of the chains in this compound can be seen in Figure 5, and this staggering of the chains gives room to accommodated the bulky TDCI ligand.

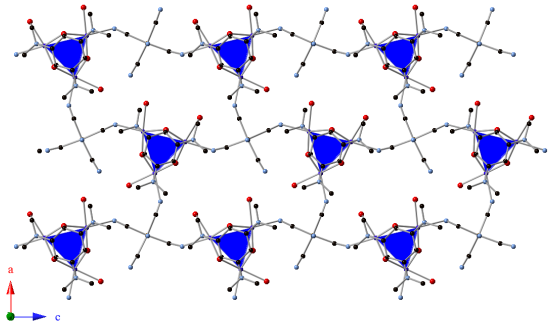


**Fig. 6** 2D-network of $[Ln_3(TDCI)_2(H_2O)_3(\mu-CN)_3Fe(CN)_3]_n$: View through the b-axis

### 3.2.2 $[Ln_3(TDCI)_2(H_2O)_3(\mu-CN)_3Fe(CN)_3]_n$

Although $[Fe(CN)]^{3-}$ is also octahedral and has the same charge as $[Cr(CN)]^{3-}$, the structures obtained with $[Fe(CN)]^{3-}$] as bridging ligand are different, featuring 2D-sheets, as shown in Figure 6. Also, in the chemistry described here, $[Fe(CN)]^{3-}$ is a more versatile linker; well-defined crystals were formed with the trinuclear lanthanide complexes containing $Gd^{3+}$, $Tb^{3+}$, $Dy^{3+}$, $Ho^{3+}$ and $Er^{3+}$. Since all of the compounds synthesized are isostructural, only compound **(4)** will be discussed, and the selected distances for the compounds in this family can be found in Table 5. The $Gd^{3+}$ ions in the trinuclear lanthanide complex are located at the vertices of a triangle, and the ligand TDCI caps the $Gd^{3+}$ ions above and below the $Gd_3$ plane, as shown in Figure 7. The three $Gd^{3+}$ ions have the same ligated atoms in their coordination environment; they are coordinated by four oxygens from four $\mu$-alkoxo groups and by two amino groups of the ligand, by one water and by a cyanido group of the linker. The $\mu_2-O-Gd$ distances range from 2.310(3) to 2.357(3)Å, which are virtually constant when compared to those of the compounds containing the linker $[Cr(CN)]^{3-}$. The $\mu_2-O-Ln$ distances decrease on moving from Gd→Er due to the lanthanide contraction. The $Gd-N$(amine) distances, range from 2.644(4) to 2.679(5) Å, and these distances moderately decrease in the congeneric compounds on going Gd→Er. The Gd−O (water) bond distances, range from 2.434(5) to 2.457(6) Å, and there is again the expected decrease in the Ln−O distances for the other compounds as Gd→Er. The distances $Gd-N$ (CN group) ranges from 2.480(6) to 2.529(7) Å, which are very close to distances previously reported,[16] and the shortening of the $Ln-NC$ bond distances is also observed for the other analogous compounds in the series Gd→Er.

The $Fe^{3+}$ ion is coordinated by six cyanide groups forming a regular octahedron. The $Fe-C$ distances range from 1.897(10) to 1.945(8) Å, and the C≡N distances range from 1.134(9) to 1.172(9) Å, which are consistent with distances previously reported.[16] The linker $[Fe(CN)_6]^{3-}$ bridges three $[Gd_3(TDCI)_2(H_2O)_3]^{3+}$ units through three cis equatorial cyanido groups, with the ∠G ranging from 142.4(8) to 150.2(9)°.

Each $[Fe(CN)_6]^{3-}$ unit is linked directly to three trinuclear lanthanide complexes, and *vice versa*, forming a "brick-like-wall" 2-D

**Table 5** $[Ln_3(TDCI)_2(H_2O)_3(\mu-CN)_3Fe(CN)_3]_n$: Selected distances (Å)

| Ln | Gd **(4)** | Tb **(5)** | Dy **(6)** | Ho **(7)** | Er **(8)** |
|---|---|---|---|---|---|
| Ln(1) - Ln(2) | 3.7051(9) | 3.6938(8) | 3.6614(6) | 3.6539(9) | 3.6273(9) |
| Ln(1) - Ln(3) | 3.7145(9) | 3.6892(7) | 3.6683(6) | 3.6478(8) | 3.6224(9) |
| Ln(2) - Ln(3) | 3.7419(8) | 3.7182(6) | 3.6973(5) | 3.6800(7) | 3.6603(7) |
| Ln(1) - O(1) | 2.450(5) | 2.427(5) | 2.403(4) | 2.392(6) | 2.371(6) |
| Ln(2) - O(2) | 2.434(5) | 2.420(5) | 2.403(4) | 2.382(6) | 2.379(5) |
| Ln(3) - O(3) | 2.457(6) | 2.444(5) | 2.429(5) | 2.413(6) | 2.410(5) |
| Ln(1) - N(1) | 2.480(6) | 2.465(6) | 2.459(5) | 2.430(8) | 2.430(6) |
| Ln(2) - N(2) | 2.529(7) | 2.507(6) | 2.496(5) | 2.470(9) | 2.468(6) |
| Ln(3) - N(3) | 2.503(6) | 2.485(6) | 2.476(5) | 2.443(8) | 2.457(6) |
| Ln(1) - O(4) | 2.336(3) | 2.316(3) | 2.304(3) | 2.289(4) | 2.282(3) |
| Ln(1) - O(5) | 2.335(4) | 2.326(3) | 2.309(3) | 2.307(4) | 2.292(3) |
| Ln(2) - O(5) | 2.325(4) | 2.324(3) | 2.308(3) | 2.298(4) | 2.284(3) |
| Ln(2) - O(6) | 2.346(3) | 2.333(3) | 2.321(3) | 2.313(4) | 2.301(3) |
| Ln(3) - O(4) | 2.310(3) | 2.298(3) | 2.286(3) | 2.261(3) | 2.258(5) |
| Ln(3) - O(6) | 2.357(3) | 2.348(3) | 2.343(3) | 2.324(3) | 2.325(5) |
| Ln(1) - N(8) | 2.679(5) | 2.681(5) | 2.666(4) | 2.662(6) | 2.665(5) |
| Ln(2) - N(6) | 2.672(5) | 2.672(4) | 2.670(5) | 2.651(5) | 2.644(5) |
| Ln(3) - N(7) | 2.644(4) | 2.622(4) | 2.622(4) | 2.600(5) | 2.604(5) |
| C(1) - N(1) | 1.156(9) | 1.148(9) | 1.153(7) | 1.135(12) | 1.158(9) |
| C(2) - N(2) | 1.134(9) | 1.166(9) | 1.157(8) | 1.172(12) | 1.159(9) |
| C(3) - N(3) | 1.172(9) | 1.159(9) | 1.163(7) | 1.168(11) | 1.154(9) |
| C(4) - N(4) | 1.171(12) | 1.143(12) | 1.152(10) | 1.138(15) | 1.146(12) |
| C(5) - N(5) | 1.142(10) | 1.153(9) | 1.146(8) | 1.146(12) | 1.140(10) |
| Fe(1) - C(1) | 1.926(8) | 1.931(8) | 1.923(6) | 1.943(12) | 1.921(7) |
| Fe(1) - C(2) | 1.945(8) | 1.924(8) | 1.930(6) | 1.919(12) | 1.935(8) |
| Fe(1) - C(3) | 1.905(8) | 1.919(8) | 1.918(6) | 1.921(11) | 1.917(8) |
| Fe(1) - C(4) | 1.897(10) | 1.921(10) | 1.918(8) | 1.936(16) | 1.920(10) |
| Fe(1) - C(5) | 1.924(8) | 1.935(7) | 1.927(6) | 1.917(10) | 1.934(8) |
| | | N···O hydrogen bond distances (Å) | | | |
| N(4) - O(1) | 2.730(10) | 2.733(10) | 2.728(8) | 2.738(13) | 2.724(10) |
| N(4) - O(3) | 2.799(11) | 2.814(10) | 2.804(9) | 2.810(14) | 2.803(10) |
| N(3) - O(2) | 3.177(9) | 3.109(8) | 3.138(6) | 3.152(10) | 3.183(7) |

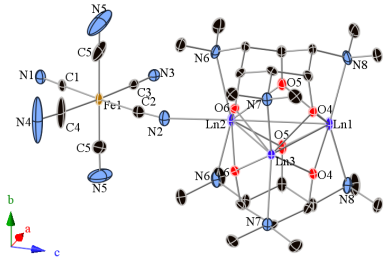


**Fig. 7** $[Ln_3(TDCI)_2(H_2O)_3(\mu-CN)_3Fe(CN)_3]$: ORTEP with 50% probability, water molecules omitted for clarity

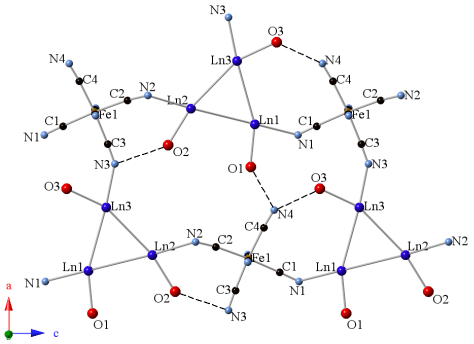


**Fig. 8** View through the b-axis of $[Ln_3(TDCI)_2(H_2O)_3(\mu-CN)_3Fe(CN)_3]$ without the ligand TDCI

network in the *a-c plane*. $[Fe(CN)_6]^{3-}$ bring the trinuclear lanthanide complexes closer, so the linker is capable of bonding to one more complex when compared with the $[Cr(CN)_6]^{3-}$ linker. The $-CN$ groups from $[Fe(CN)_6]^{3-}$ form hydrogen bonds with the coordinated waters of the $Gd^{3+}$ ions as seen in Figure 8, and this hydrogen bonding helps to stabilize the 2D-network formed. The $d(N\cdots O)$ hydrogen bond range from 2.730(10) to 3.177(9) Å, which fall in the range of a 'moderate' strength.[33] Hydrogen bonding for each of the compounds are summarized in Table 5.

The compounds of this family are also characterized by showing a degree of higher disorder of the 'free' cyanido groups due to vibration caused by hydrogen bonding to water molecules. The packing of the layers in this family is characterized by having a hydrophobic interlayer interaction as depicted in Figure 9.

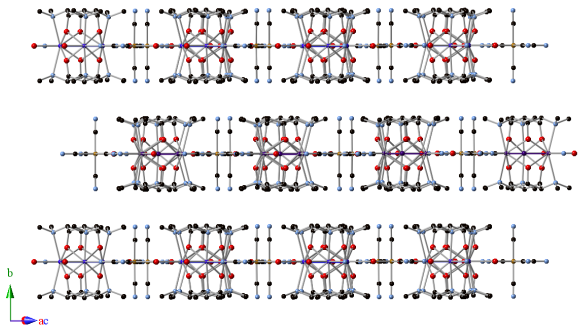


**Fig. 9** [1,0,-1] view of $[Ln_3(TDCI)_2(H_2O)_3(\mu-CN)_3Fe(CN)_3]_n$

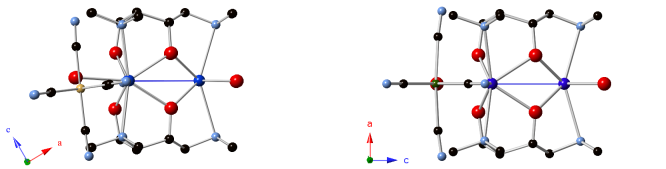

**(a)** $[Ho_3(TDCI)_2(H_2O)_4Co(\mu-CN)_2(CN)_4]$ **(b)** $[Dy_3(TDCI)_2(H_2O)_4Cr(\mu-CN)_2(CN)_4]$

**Fig. 10** Side view of the complexes showing the torsion angle

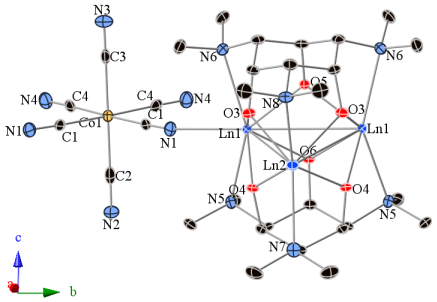


**Fig. 11** ORTEP drawing with 50% probability of $[Ln_3(TDCI)_2(H_2O)_4Co(\mu-CN)_2(CN)_4]$ without water for clarity

### 3.2.3 $[Ln_3(TDCI)_2(H_2O)_4Co(\mu-CN)_2(CN)_4]_n$

The compounds formed using $[Co(CN)_6]^{3-}$ and $[Ln_3(TDCI)_2(H_2O)_4]^{3+}$ (Ln = $Ho^{3+}$, $Er^{3+}$ and $Y^{3+}$) feature chains of alternating units of the linker and trinuclear lanthanide complexes. These compounds are very similar to those obtained with the linker $[Cr(CN)_6]^{3-}$. However, one of the differences between these two families of compounds is that the equatorial cyanido groups of the $[Cr(CN)_6]^{3-}$ are coplanar to the $Ln_3$ plane while $[Co(CN)_6]^{3-}$ shows a torsion angle from the $Ln_3$ plane as seen in Figure 10. The dihedral angle observed between the lanthanide plane and the linker for $Ho^{3+}$, $Er^{3+}$ and $Y^{3+}$ compounds are similar, 5.823°, 4.723°and 6.156°, respectively.

Since the three compounds synthesized are isostructural, only compound **(10)** will be discussed; the interatomic distances for the compounds in this family are summarized in Table 6. The $Ho^{3+}$ ions in the trinuclear lanthanide complex are located at the vertices of a triangle, and the TDCI ligand caps the $Ho^{3+}$ ions above and below the plane in which the three $Ho^{3+}$ ions are contained as shown in Figure 11. The $Ho(1)^{3+}$ ion is coordinated by four oxygens from four $\mu$-alkoxo groups and by two amino groups of the ligand, by one water and by a cyanido group of the linker. The $\mu_2-O(5)-Ho(1)$ and $\mu_2-O(6)-Ho(1)$ bond distances are 2.2712(19) and 2.2815(19) Å, respectively, and the Ho(1) − N(1) (CN group) distance is 2.440(3) Å. The bond distances of Ho(1)−O(1), water coordinated to the ion, is 2.405(3) Å. The bond distances Ho(1)−N (amine) are 2.640(3) and 2.645(3) Å.

The coordination around $Ho(2)^{3+}$ ion is similar to that of $Ho(1)^{3+}$ ion except that $Ho(2)^{3+}$ ion has two water molecules

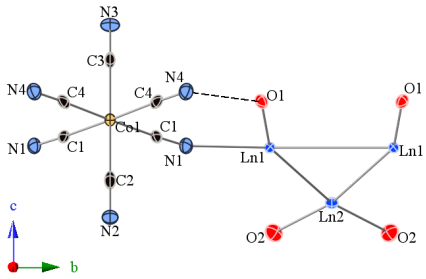


**Fig. 12** Thermal ellipsoid drawing with 50% probability of $[Ln_3(TDCI)_2(H_2O)_4(\mu-CN)_2Co(CN)_4]$ without the ligand TDCI

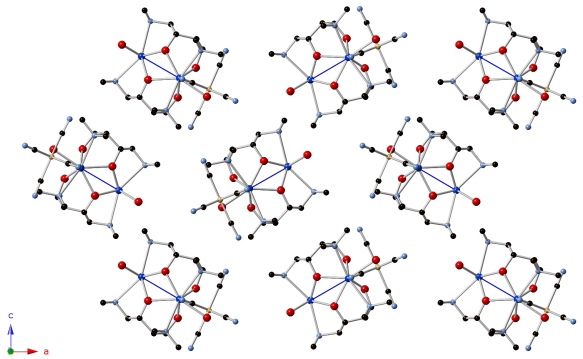


**Fig. 13** b-axis view of $[Ln_3(TDCI)_2(H_2O)_4(\mu-CN)_2Co(CN)_4]_n$

coordinated instead of a cyanido group, as shown in Figure 11. The bond distances of $\mu_2-O(3)-Ho(2)$ and $\mu_2-O(4)-Ho(2)$ are 2.315(2) and 2.307(2) Å, respectively. The bond distance of Ho(2)−O(2), water coordinated to the ion, is 2.405(3) Å, and the bond distances Ho(2)−N, the amino group of the ligand, are 2.646(4) and 2.647(4) Å.

The shorter $\mu_2-O-Ho(2)$ distances observed around the ion can be interpreted as consequence of the weaker donors at the other coordination sites around this ion. Since the cyanido ligand is not as good electron donor as water, the alkoxo groups from TDCI move closer to donate more electron density. A compensation elongation of $\mu_2-O-Ho(1)$ bond distances can be seen as well. The coordinated water to the $Ho(1)^{3+}$ ion moves closer to compensate for the small shifting of the alkoxo groups of the ligand. The bond distances found for this compound are close to those obtained in $[Ho_3(TDCI)_2(H_2O)_3(\mu-CN)_3Fe(CN)_4]$.

The $Co^{3+}$ ion is coordinated by six cyanide groups forming a regular octahedron. The Co − C distances range from 1.879(4) to 1.913(6) Å, which are consistent with the distances previously reported.[16] $[Co(CN)_6]^{3-}$ links two $[Ho_3(TDCI)_2(H_2O)_4]^{3+}$ tectons through two cyanido groups, ∠Ho(1)N(1)C(1) = 142.6(4)°; the $Ho^{3+}$ ions of the trinuclear lanthanide complexes involved in the linkage, $Ho(1)^{3+}$ - $Ho(1)^{3+}$, can be seen as the base of the triangles. Each $[Co(CN)_6]^{3-}$ unit bridges two trinuclear lanthanide complexes resulting in a 1-D chain of alternating units of linker and trinuclear lanthanide complex that grows along the *b axis*. Similar to the chains obtained with $[Cr(CN)_6]^{3-}$, the lanthanide

**Table 6** $[Ln_3(TDCI)_2(H_2O)_4(\mu-CN)_2Co(CN)_4]_n$: Selected distances (Å)

| Ln | Ho **(9)** | Er **(10)** | Y **(11)** |
|---|---|---|---|
| Ln(1) - Ln(1) | 3.5989(7) | 3.5828(14) | 3.595(2) |
| Ln(1) - Ln(2) | 3.6873(5) | 3.6723(10) | 3.6871(14) |
| Ln(1) - O(1) | 2.405(3) | 2.407(3) | 2.4115(19) |
| Ln(2) - O(2) | 2.365(3) | 2.360(3) | 2.367(2) |
| Ln(1) - N(1) | 2.440(3) | 2.422(5) | 2.446(3) |
| Ln(1) - O(3) | 2.324(2) | 2.308(4) | 2.3161(19) |
| Ln(1) - O(4) | 2.316(2) | 2.316(3) | 2.326(2) |
| Ln(1) - O(5) | 2.2712(19) | 2.264(3) | 2.2853(16) |
| Ln(1) - O(6) | 2.2815(19) | 2.277(3) | 2.2724(16) |
| Ln(2) - O(3) | 2.315(2) | 2.308(3) | 2.3093(19) |
| Ln(2) - O(4) | 2.307(2) | 2.294(3) | 2.3107(19) |
| Ln(1) - N(5) | 2.640(3) | 2.638(4) | 2.651(2) |
| Ln(1) - N(6) | 2.645(3) | 2.644(4) | 2.644(2) |
| Ln(2) - N(7) | 2.646(4) | 2.638(6) | 2.650(3) |
| Ln(2) - N(8) | 2.647(4) | 2.652(6) | 2.656(3) |
| C(1) - N(1) | 1.159(5) | 1.162(7) | 1.154(3) |
| C(2) - N(2) | 1.157(7) | 1.143(9) | 1.150(5) |
| C(3) - N(3) | 1.150(7) | 1.158(9) | 1.154(5) |
| C(4) - N(4) | 1.152(5) | 1.160(7) | 1.158(3) |
| Co(1) - C(1) | 1.879(4) | 1.888(6) | 1.883(3) |
| Co(1) - C(2) | 1.913(6) | 1.931(8) | 1.917(4) |
| Co(1) - C(3) | 1.909(6) | 1.915(8) | 1.918(4) |
| Co(1) - C(4) | 1.898(4) | 1.894(6) | 1.890(3) |
| | N···O hydrogen bond distances (Å) | | |
| N(4) - O(1) | 3.035(5) | 3.032(6) | 3.029(3) |

complexes show hydrogen bonding of 'moderate' strength[33] between the water coordinated to the $Ho(1)^{3+}$ ion and the nitrogen from the cyanido group, $O(1)\cdots N(4)$, with a distance of 3.076(5) Å as seen in Figure 12.

### 3.3 Magnetic properites

The magnetic susceptibility measurements of compounds **(1)** - **(3)** are depicted in Figure 14, and the dashed lines represent the expected Curie behavior for three independent $Ln^{3+}$ ions and one $Cr^{3+}$ ion ($S = 3/2$, $^4A_2$). As it has been previously described, any deviation in the $\chi_m T$ values from the expected Curie behavior indicates the net magnetic coupling among the ions.[34] The experimental $\chi_m T$ values for compounds **(1)** - **(3)** approach the expected Curie behavior for magnetically independent ions at T > 100 K, thus, indicating that they do not show ferromagnetic coupling. Additionally, experimental Curie and Weiss constants were obtained for each compound by fitting all the data using the Curie-Weiss equation $[1/\chi_m = (T-\theta)/C_m]$, and their values are all summarized in Table 7.

The experimental $C_m$ values, which are very close to the theoretical $C_m$, confirm that the compounds exhibit the magnetically independent behavior of their constituting ions. However, it is not clear if the nature of the negative values of the Weiss constants arises solely from antiferromagnetic interactions or, except for $Gd^{3+}$ ions, due to spin-orbit coupling effects from the lanthanide ions within the trinuclear lanthanide complexes. Although the magnetic behavior of compound **(1)** originates from a spin pure magnetic core $[Gd_3Cr]$ and spin-orbit contributions are not observed, it is still not evident if the declining $\chi$T values at T < 100 K originate from antiferromagnetic interactions due to spin reversal within the same chain or due to interchain interactions.[35]

Furthermore, magnetization measurements at 1.8 K for com-

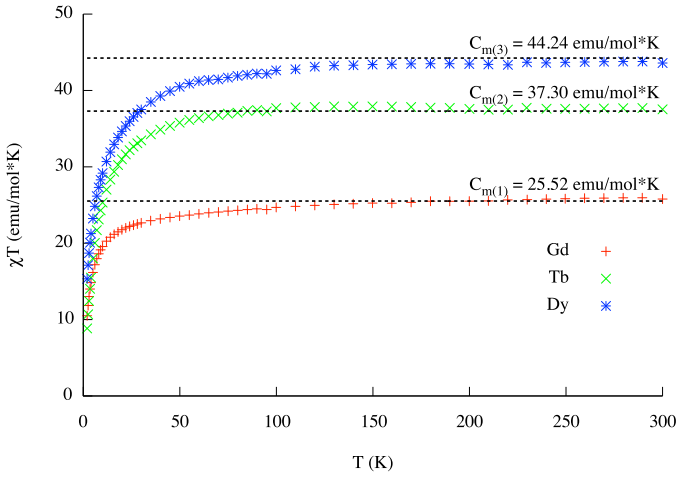


**Fig. 14** Magnetic susceptibility for the family of compounds $[Ln_3(TDCI)_2(H_2O)_4(\mu-CN)_2Cr(CN)_4]_n$. The dashed lines represent the expected Curie behavior for each compound.

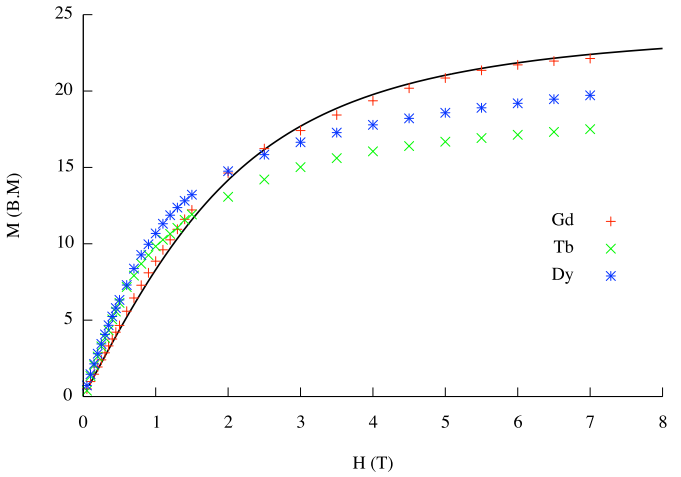


**Fig. 15** Magnetization at 1.8 K for the family of compounds $[Ln_3(TDCI)_2(H_2O)_4(\mu-CN)_2Cr(CN)_4]_n$. The solid line represents the Brillouin function for three uncorrelated $Gd^{3+}$ ions and a $Cr^{3+}$ ion.

**Table 7** Experimental and theoretical Curie constant for the $[Ln_3M]$ core of the the selected compounds

| Compound | Ln Ground State | $C_m$ (emu/mol*K) Theoretical | $C_m$ (emu/mol*K) Experimental | $\theta$ (K) |
|---|---|---|---|---|
| (1) $[Gd_3Cr]$ | $^8S_{7/2}$ | 25.52 | $26.16 \pm 0.05$ | $-4.47 \pm 0.25$ |
| (2) $[Tb_3Cr]$ | $^7F_6$ | 37.30 | $38.45 \pm 0.08$ | $-4.38 \pm 0.29$ |
| (3) $[Dy_3Cr]$ | $^6H_{15/2}$ | 44.24 | $44.56 \pm 0.04$ | $-4.99 \pm 0.12$ |
| (6) $[Dy_3Fe]$ | $^6H_{15/2}$ | 43.00 | $43.78 \pm 0.12$ | $-5.61 \pm 0.37$ |
| (7) $[Ho_3Fe]$ | $^5I_8$ | 42.76 | $43.19 \pm 0.13$ | $-9.60 \pm 0.44$ |
| (8) $[Er_3Fe]$ | $^6I_{15/2}$ | 34.95 | $36.80 \pm 0.11$ | $-5.03 \pm 0.45$ |

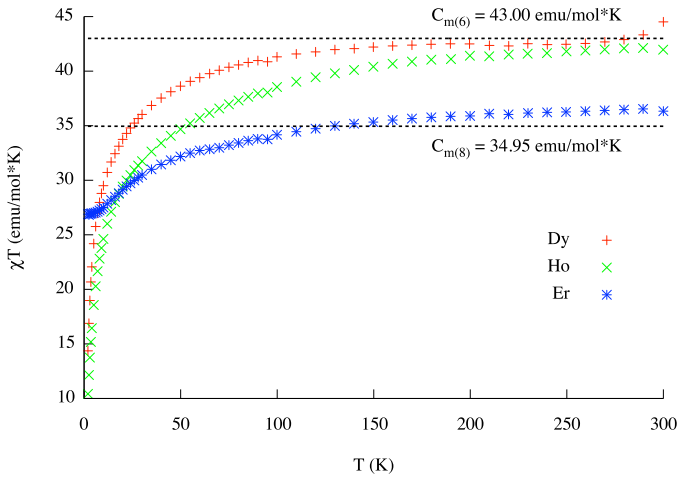


**Fig. 16** Magnetic susceptibility for the family of compounds $[Ln_3(TDCI)_2(H_2O)_3(\mu-CN)_3Fe(CN)_3]_n$. The dashed lines represent the expected Curie behavior for each compound.

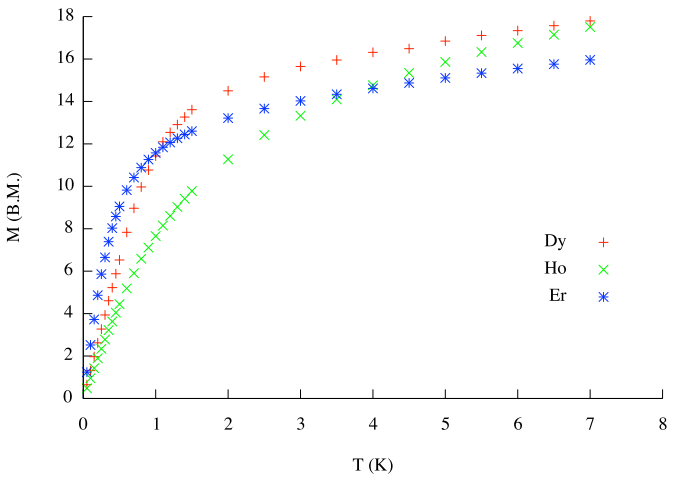


**Fig. 17** Magnetization at 1.8 K for the family of compounds $[Ln_3(TDCI)_2(H_2O)_4(\mu-CN)_2Cr(CN)_4]_n$

pounds **(1)** - **(3)** confirm that their magnetic behavior is due to the presence of uncorrelated $Ln^{3+}$ and $Cr^{3+}$ ions. In Figure 15, the solid line correspond to the Brillouin function for three uncoupled $Gd^{3+}$ and $Cr^{3+}$ ions, and the experimental magnetization for compound **(1)** does not differ much from its theoretical magnetization behavior. For compounds **(2)** and **(3)**, crystal-field effects are expected to reduce the magnetization; for example, the magnetization at 7 T for one $Dy^{3+}$ ion is expected to be $5.23\mu_B$.[36] Taking into account the magnetic contribution of the $Cr^{3+}$ ion, the experimental magnetization obtained for compound **(3)** reveal a magnetization of $5.57\mu_B$ per $Dy^{3+}$ ion at 7T, which is close to the reported value. Even though the magnetization behavior of compound **(2)** gets complicated by crystal-field effects, at low magnetic fields (H < 1T), the experimental magnetization is consistent to the expected magnetization for three uncorrelated $Tb^{3+}$ and $Cr^{3+}$ ions.

Magnetic susceptibility and magnetization measurements, Figure 16 and Figure 17, respectively, were also performed on compounds **(6)** - **(8)**. The magnetic behavior for compounds **(6)** and **(7)** show that there is not a net magnetic coupling among their ions. However, the magnetic susceptibility of compound **(8)** surpasses the expected Curie behavior at T > 150 K, and instead of tending to zero at low temperatures, its $\chi T$ values tend to $\approx 27$ emu/mol*K. Additionally, the experimental magnetization at H < 1 T is larger than the expected magnetization for three independent $Er^{3+}$ ions and a $Fe^{3+}$ ion, thus, suggesting the presence of possible intra ferromagnetic coupling of the trinuclear lanthanide cluster. In order to better understand the nature of the magnetic behavior of compound **(8)**, more detailed magnetic studies and *ab initio* calculations are required.[37]

## 4 Conclusion

The use of trinuclear lanthanide complexes supported by TDCI coupled with the versatility of the cyanido groups of the hexacyanometallates to bridge two or three lanthanide tectons yield a variety of unexpected structures, even though the molecular shape and the charges are the same for all of the hexacyanometallates.

There exists an intrinsic relationship between the size of the linker and the size of the ions in the trinuclear lanthanide complexes. Crystals were obtained when the larger linker $[Cr(CN)_6]^{3-}$ was combined with trinuclear lanthanide complexes having the larger ions $Gd^{3+}$, $Tb^{3+}$ and $Dy^{3+}$, but crystals did not form when the trinuclear lanthanide complexes had the smaller ions $Ho^{3+}$, $Er^{3+}$ and $Y^{3+}$. In contrast, the smaller linker $[Co(CN)_6]^{3-}$ produced crystals when the trinuclear lanthanide complexes had the smaller ions $Ho^{3+}$, $Er^{3+}$ and $Y^{3+}$, but crystals were not formed when the trinuclear lanthanide complexes contained the larger ions $Gd^{3+}$, $Tb^{3+}$ and $Dy^{3+}$. Moreover, in the chemical context reported here, $[Fe(CN)_6]^{3-}$ has shown to be a more versatile linker, for crystals were obtained when the trinu-

clear lanthanide complexes contained $Gd^{3+}$ - $Er^{3+}$ ions, but not with $Y^{3+}$.

The family obtained with the linker $[Cr(CN)_6]^{3-}$ has three isostructural compounds when the trinuclear lanthanide complex has the lanthanide ions $Gd^{3+}$, $Tb^{3+}$ and $Dy^{3+}$. This family of compounds features 1-D chains of alternating units of the linker and the trinuclear lanthanide complexes. The linker bridges two trinuclear lanthanide complexes through two cis cyanido groups, and all of the compounds in this family crystallize in the *Pmmn* space group.

Despite the close similarity of $[Fe(CN)_6]^{3-}$ and $[Cr(CN)_6]^{3-}$, compounds synthesized with the two different linkers differ in their structures. $[Fe(CN)_6]^{3-}$ bridges three trinuclear lanthanide complexes forming a 2D-network, and all of the compounds in this family crystallize in the *Pnma* space group.

Unexpectedly, $[Co(CN)_6]^{3-}$ gives yet another family of three isostructural compounds when the trinuclear lanthanide complex contains $Ho^{3+}$, $Er^{3+}$ and $Y^{3+}$. These compounds form 1-D chains of alternating linker molecules and trinuclear lanthanide complex units, similarly to the compounds having $[Cr(CN)_6]^{3-}$. However, they crystallize in the *Pnma* space group, and $[Co(CN)_6]^{3-}$ is not coplanar to the trinuclear lanthanide complex forming a torsion angle.

Magnetic susceptibility and magnetization measurements of the selected compounds show that their magnetic behavior is that of their constituent ions, except for $[Er_3(TDCI)_2(H_2O)_3(\mu-CN)_3Fe(CN)_3]_n$. For compounds **(1)** - **(3)** and **(6)** - **(7)**, their $\chi T$ values do not surpass the expected Curie behavior, and the $C_m$ constants obtained by fitting the data are very close to the expected $C_m$ values of each compound. The magnetization behavior of compound **(1)** fits the expected behavior for three $Gd^{3+}$ ions and one $Cr^{3+}$ ion, confirming that there is not a net magnetic coupling. Even though crystal-field effects are reflected in the magnetization measurements of compounds **(2)**, **(3)**, **(6)** and **(7)**, at H < 1 T, their magnetization corresponds to that of uncorrelated ions. The magnetic behavior of compound **(8)** suggest the presence of ferromagnetic coupling, but more detailed studies are required to better understand the interaction of the $Er^{3+}$ ions in the trinuclear lanthanide complex.

## Acknowledgements

We thank the Texas Advanced Research Program through Grant 010366-0188-2001. We also thank the X-ray Diffraction Laboratory at the Department of Chemistry, Texas A & M University which diffractometers and crystallographic computing systems are funded by the National Science Foundation (CHE-9807975, CHE-0079822 and CHE-0215838). We also thank the SQUID facility at Texas A&M University for facilitating the acquisition of magnetic data. The MPMS-XL Quantum Design SQUID magnetometer was purchased by funds provided by the NSF (CHE-9974899). The MPMS-3 Quantum Design SQUID magnetometer was purchased by funds provided by Texas A & M University Vice President of Research.

## References

1 S. Liu, C. E. Plecnik, E. A. Meyers and S. G. Shore, *Inor. Chem.*, 2005, **44**, 282–292.
2 G. Li, T. Akitsu, O. Sato and Y. Einaga, *J. Am. Chem. Soc.*, 2003, **125**, 12396–12397.
3 H. Svendsen, J. Overgaard, M. Chevallier, E. Collet, Y.-S. Chen, F. Jensen and B. Iversen, *Chem. Eur. J.*, 2010, **16**, 7215–7223.
4 F. Renaud, C. Piguet, G. Bernardinelli, J.-C. G. Bünzli and G. Hopfgartner, *Chem. Eur. J.*, 1997, **3**, 1646–1659.
5 Y. Guo, G.-F. Xu, C. Wang, T.-T. Cao, J. Tang, Z.-Q. Liu, Y. Ma, S.-P. Yan, P. Cheng and D.-Z. Liao, *Dalton Trans.*, 2012, **41**, 1624–1629.
6 G. M. Davies, S. J. A. Pope, H. Adams, S. Faulkner and M. D. Ward, *Inor. Chem.*, 2005, **44**, 4656–4665.
7 M. Andruh, J.-P. Costes, C. Diaz and S. Gao, *Inor. Chem.*, 2009, **48**, 3342–3359.
8 S. Liu, P. Poplaukhin, E. Ding, C. E. Plecnik, X. Chen, M. A. Keane and S. G. Shore, *J. Alloys Compd.*, 2006, **418**, 21 – 26.
9 P. Przychodzen, K. Lewinski, R. Pelka, M. Balanda, K. Tomala and B. Sieklucka, *Dalton Trans.*, 2006, 625–628.
10 W.-F. Yeung, T.-C. Lau, X.-Y. Wang, S. Gao, L. Szeto and W.-T. Wong, *Inor. Chem.*, 2006, **45**, 6756–6760.
11 D.-Y. Yu, L. Li, H. Zhou, A.-H. Yuan and Y.-Z. Li, *Eur. J. Inorg. Chem.*, 2012, **2012**, 3394–3397.
12 S. Tanase and J. Reedijk, *Coord. Chem. Reviews*, 2006, **250**, 2501 – 2510.
13 X. Zhao, X.-Y. Yu, T.-L. Chen, Y.-H. Luo, J.-J. Yang and H. Zhang, *Inor. Chem. Commun.*, 2012, **20**, 247 – 251.
14 S. Tanase, M. Andruh, A. Muller, M. Schmidtmann, C. Mathoniere and G. Rombaut, *Chem. Commun.*, 2001, 1084–1085.
15 D. Visinescu, O. Fabelo, C. Ruiz-Perez, F. Lloret and M. Julve, *Cryst. Eng. Comm.*, 2010, **12**, 2454–2465.
16 W.-T. Chen, A.-Q. Wu, G.-C. Guo, M.-S. Wang, L.-Z. Cai and J.-S. Huang, *Eur. J. Inorg. Chem.*, 2010, **2010**, 2826–2835.
17 E. Chelebaeva, J. Larionova, Y. Guari, R. A. S. Ferreira, L. D. Carlos, F. A. A. Paz, A. Trifonov and C. Guérin, *Inor. Chem.*, 2009, **48**, 5983–5995.
18 Y.-Z. Zhang, G.-P. Duan, O. Sato and S. Gao, *J. Mater. Chem.*, 2006, **16**, 2625–2634.
19 R. Koner, M. G. Drew, A. Figuerola, C. Diaz and S. Mohanta, *Inor. Chim. Acta*, 2005, **358**, 3041 – 3047.
20 H. Zhou, Q. Chen, H.-B. Zhou, X.-Z. Yang, Y. Song and A.-H. Yuan, *Cryst. Growth Des.*, 2016, **16**, 1708–1716.
21 X.-J. Song, J.-J. Xu, Y. Chen, M. Muddassir, F. Cao, R.-M. Wei, Y. Song and X.-Z. You, *Polyhedron*, 2013, **66**, 212 – 217.
22 T. Kradolfer and K. Hegetschweiler, *Hel. Chim. Acta*, 1992, **75**, 2243–2251.
23 M. W. Hosseini, *Cryst. Eng. Comm.*, 2004, **6**, 318–322.
24 S. Mann, *Nature*, 1993, **365**, 499–505.
25 M. Simard, D. Su and J. D. Wuest, *J. Am. Chem. Soc.*, 1991, **113**, 4696–4698.
26 K. Hegetschweiler, I. Erni, W. Schneider and H. Schmalle,

*Helv. Chim. Acta*, 1990, **73**, 97–105.
27 M. Ghisletta, K. Hegetschweiler, H.-P. Jalett, T. Gerfin and V. Gramlich, *Helv. Chim. Acta*, 1992, **75**, 2233–2242.
28 Bruker, *(2012) Bruker AXS Inc., Madison, Wisconsin, USA.*
29 G. M. Sheldrick, *(1996) University of Göttingen, Germany*.
30 O. V. Dolomanov, L. J. Bourhis, R. J. Gildea, J. A. K. Howard and H. Puschmann, *J. Appl. Crys.*, 2009, **42**, 339–341.
31 G. M. Sheldrick, *Acta Crys. A*, 2008, **64**, 112–122.
32 G. A. Bain and J. F. Berry, *J. Chem. Educ.*, 2008, **85**, 532.
33 G. A. Jeffrey, *An Introduction to Hydrogen Bonding*, Oxford University Press, 1997.
34 L. E. Sweet, L. E. Roy, F. Meng and T. Hughbanks, *J. Am. Chem. Soc.*, 2006, **128**, 10193–10201.
35 L. Bogani, A. Vindigni, R. Sessoli and D. Gatteschi, *J. Mater. Chem.*, 2008, **18**, 4750–4758.
36 J. Tang, I. Hewitt, N. T. Madhu, G. Chastanet, W. Wernsdorfer, C. E. Anson, C. Benelli, R. Sessoli and A. K. Powell, *Angew. Chem. Int. Ed.*, 2006, **45**, 1729–1733.
37 L. Sorace, C. Sangregorio, A. Figuerola, C. Benelli and D. Gatteschi, *Chem. Eur. J.*, 2009, **15**, 1377–1388.

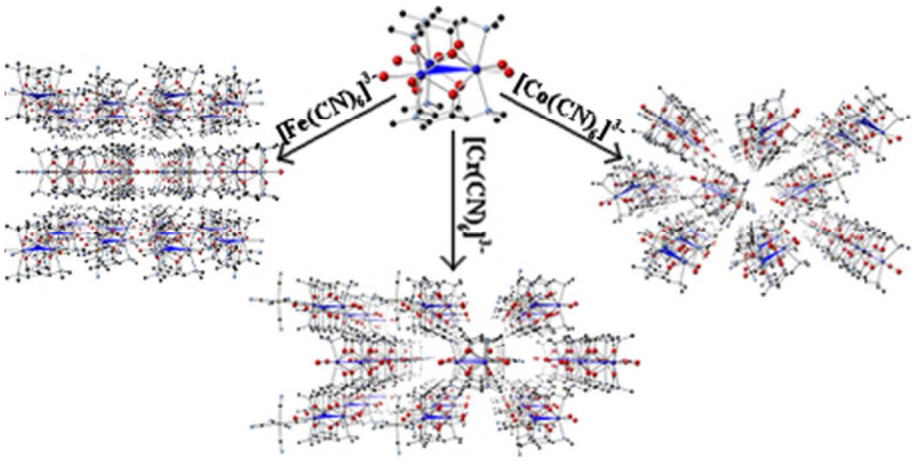


80x40mm (144 x 144 DPI)